

Architecture of left-handed metamaterial absorber for absorbing electromagnetic hazards

M. R. I. FARUQUE^{a,*}, M. RAHMAN^b, M. M. HASAN^a, A. M. TAMIM^a, I. N. IDRUS^a, M. T. ISLAM^c

^aSpace Science Centre (ANGKASA), Universiti Kebangsaan Malaysia, Bangi 43600, Malaysia

^bDepartment of Electronics and Communication Discipline, Khulna University, Khulna, Bangladesh

^cDepartment of Electrical, Electronic and Systems Engineering, Universiti Kebangsaan Malaysia, Bangi 43600, Malaysia

At present because of extensive space and environmental radiation research, we have a much better understanding of our space and earth environment, its effects, and the best ways to protect the human life. Besides, with the increase in the environmental issues caused by traditional resources, renewable energy has attracted worldwide attention nowadays by suppression of unwanted radiation produced by devices in space/climate. An electric-inductive-capacitive resonator that are capable of not only suppression of unwanted microwave radiation but also channelling almost all the absorbed power to a resistive load was discussed in this paper. The proposed absorber structure shows a wide bandwidth of 4.66 GHz, whereas the size of every unit cell was $10 \times 10 \text{ mm}^2$ and total array slab was $150 \times 200 \text{ mm}^2$. Finite integration technique (FIT) based CST Microwave Studio was used for design and analyses purpose. The measured result shows resonance in 4.16 GHz (C-band), 8.18 GHz (X-band), 12.03 GHz (Ku-band), 16.61 GHz (Ku-band) and the effective medium ratio is 7.21. However, the absorption of the proposed metamaterial absorber at 2.06, 5.05, 9.26, and 13.23 GHz were respectively, 60%, 95%, 78%, and 93%.

(Received April 7, 2019; accepted October 22, 2020)

Keywords: Absorption, Electromagnetic hazards, Left-handed metamaterial, Renewable energy

1. Introduction

For communication, systems used in everyday life, such as cellular telephones, mobile communication equipment, satellite TV, radiation of the domestic microwave ovens presents a severe electromagnetic compatibility (EMC) problem. Widely used such microwave devices have an essential shortcoming: besides the primary oscillation, the magnetron has unwanted electromagnetic radiation in the region of 1.0 to 18.0 GHz. Metamaterials have attracted extensive attention from the year. The explosion of interest is due to the dramatically physical properties for sound, elastic and EM-waves, which are not available in natural materials. At present, these artificial material has been used for antenna performance enhance, cloaking, electromagnetic absorption applications. Therefore, some of the applications of electromagnetic absorber for absorbing unwanted hazards in climate and space by attaching the metamaterial on the surface or insides the regular commercial devices and satellites.

Landy et al. in 2008 introduced the first perfect metamaterial absorber, which achieved its peak absorption of 88% at 11.5 GHz [3]. In addition, the possible health risk caused by mobile handsets due to their electromagnetic interaction with the user's head. There is a significant need to evaluate electromagnetic absorption by the human head during the uses of electronic devices such as mobile phones [4-5]. A quad-band terahertz absorber is suggested, which consisted of two different sizes periodic array of the split ring resonators, and the results indicate that average absorption was around 96% [6].

Moreover, after reducing the coupling, capacitance in the z-axis absorption was reached up to 55% introduced by Islam et al. [7]. An absorber was composed of delicate periodic patterned and metallic background plane structures and exhibited absorption rates above 99% for four absorption peaks in 2015 [8]. Hasan et al. introduced a chiral metamaterial which displayed resonance at C-band and 5.14 GHz bandwidth from 4.0 to 9.14 GHz [9]. Swallow et al. developed a micropower generator device consisted of piezoelectric fibres, $90 \mu\text{m}$ to $250 \mu\text{m}$ in diameter, and shown voltage output up to 6.0 V [10]. A group of researchers suggested a new type of particles that can act as energy collectors when a resistive load was inserted within the particle's gap. They considered an $85.0 \times 85.0 \text{ mm}^2$ footprint occupied by a 9×9 split ring resonator array resulting in a total of 81 split ring resonator cells in 2012 [11]. In 2015, a selective solar absorber was proposed, and the solar absorber was characterised to be higher than 0.9 [12]. In [13] a microwave metamaterial absorber was introduced, which showed resonances at C-, X- and Ku-band with double negative characteristics as well as the absorption peaks were respectively, 82%, 67%, and 93% at 6.22, 8.76, and 13.05 GHz. Almoneef et al. presented a metamaterial slab comprised of 13×13 electrically small cells, each loaded with an 82Ω resistor. The designed structure shown power absorption efficiency of 97% and 93%, respectively, in 2015 [14]. Apart from that, the different researcher proposed and developed numerous microwave [15-16] and terahertz absorbers [17-20] for different sort of applications, and the research is going to a never-ending way.

In this paper, a metamaterial harvester harvesting

energy by absorbing harmful hazards in the microwave regime. The size of every unit cell of the absorber slab is $10 \times 10 \text{ mm}^2$. The measured result show resonance in 4.16 GHz (C-band), 8.18 GHz (X-band), 12.03 GHz (Ku-band), 16.61 GHz (Ku-band) and the effective medium ratio is 7.21. The absorber has the absorption capacity of 60% at 2.06 GHz, absorption capacity of 95% at 5.05 GHz, the absorption capacity of 78% at 9.26 GHz, and absorption capacity of 93% at 13.23 GHz.

2. Design of the metamaterial absorber

To describe the schematic, fabricated prototype clearly and the parameters of the designed absorber structure are shown in Fig. 1(a-c).

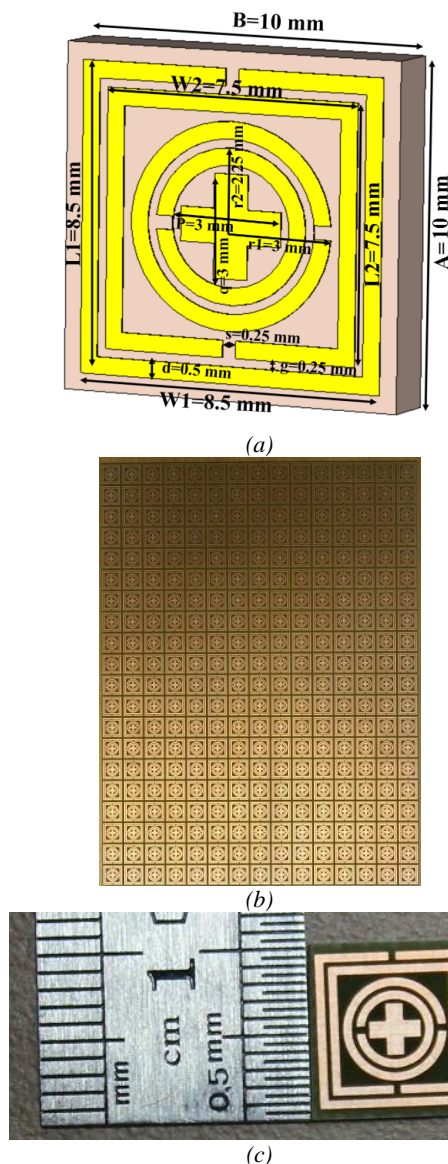


Fig. 1. Proposed metamaterial absorber: (a) Schematic view; Fabricated: (b) array structure and (c) unit cell (color online)

The designed structure consists of square outer and

inner metallic resonators, where the circular rings are in the centre of the inner resonator. There is splits in every resonator and the circular metallic rings, which formed the capacitance and shifted the resonance points toward higher frequency. The proposed metallic absorber structure was printed on FR-4 dielectric substrate material. Copper was used as a resonator on the dielectric substrate with an electrical conductivity of $\sigma = 5 \times 8 \text{ s/m}$.

The dimensions of the metamaterial absorber unit cell structure are: $A = 10.0 \text{ mm}$, $B = 10.0 \text{ mm}$, $L_1 = 8.5 \text{ mm}$, $W_1 = 8.5 \text{ mm}$, $L_2 = 7.5 \text{ mm}$, $W_2 = 7.5 \text{ mm}$, $r_1 = 3.0 \text{ mm}$, $r_2 = 1.25 \text{ mm}$, $P = 3.0 \text{ mm}$, $d = 0.5 \text{ mm}$, and $g = 0.25 \text{ mm}$.

3. Methodology and measurement

To understand and characterise the absorption mechanism of the proposed left-handed absorber simulations was performed through CST Microwave Studio simulator that uses the finite integration technique. In the simulation, the electric and magnetic field components of the incident plane wave are parallel to the x- and y-direction, as well as the direction of incident wave propagation, is z-direction. Frequency-domain solver in CST-MWS was used to retrieve the effective parameters, which are given as follows [21],

$$S_{11} = \left\{ \frac{R_1(1 - e^{jnk d})}{1 - R_1^2 e^{jnk d}} \right\} \quad (1)$$

$$\text{Similarly, } S_{21} = \left\{ \frac{e^{jnk d}(1 - R_1^2)}{1 - R_1^2 e^{jnk d}} \right\} \quad (2)$$

$$k \approx \frac{1}{jd} \times \frac{(1 - S_{21} - S_{11})(1 + R_1)}{1 - R_1(S_{21} + S_{11})} \quad (3)$$

Refractive index,

$$n = \frac{2}{jkd} \sqrt{\frac{(S_{21} - 1)^2 - S_{11}^2}{(S_{21} + 1)^2 - S_{11}^2}} \quad (4)$$

Effective permittivity,

$$\epsilon_r = (n/Z) \quad (5)$$

Effective permeability,

$$\mu_r = (n \times Z) \quad (6)$$

Moreover, the reactance impedance is directly extracted from the reflection and transmission coefficient to prove the proposed design as a metamaterial structure. The reflection and transmission are related to the impedance of the periodic metamaterial for the normally incident plane wave can be expressed as,

Reactance Impedance,

$$Z_{ms} = \left\{ \frac{2n(1-S_{21}+S_{11})}{(1+S_{21}-S_{11})} \right\} \quad (7)$$

Electromagnetic absorption behaviour can be calculated by using Eq. (8), where $A(f)$, $R(f)$, and $T(f)$ represent the absorption, respectively, reflectance and transmittance of the proposed absorber. Using Eq. (9) the scattering parameters from the simulation can obtain absorption characteristics,

$$A(f) = [1 - R(f) - T(f)] \quad (8)$$

Absorption,

$$A(f) = [1 - |S_{11}|^2 - |S_{21}|^2] \quad (9)$$

For the measurement of the proposed metamaterial structure, an array prototype was fabricated, and the array prototype was placed in front of the horn antenna, as shown in Fig. 1(b). The signal generator generates the EM-wave, whereas the EM-wave propagates along z-directions to an incident on the metamaterial structure (shown in Fig. 2(b)). Besides, an Agilent N5227A vector network analyser was utilised to investigate the scattering and effective medium parameter results shown in figure 2(a). However, an Agilent N4694-60001 was used for calibration the N5227A VNA to perform the measurement accurately,

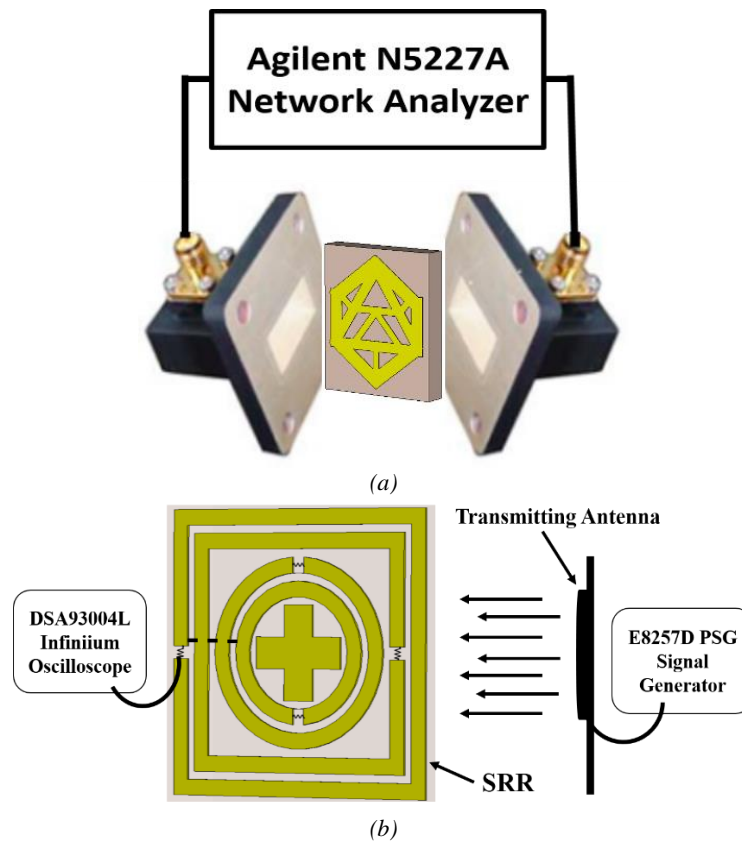


Fig. 2. Measurement procedure of the: (a) Scattering parameters, and (b) Induced voltage across the resistor placed between the splits of the proposed metamaterial absorber structure (color online)

4. Result analysis

The behaviour of the metamaterial absorber can be analysed by the electric field, magnetic field, and surface current distributions, as presented in Fig. 3(a-d). Electric field distribution shows charge accumulation on the oppositely facing strips and indicates the capacitive effect. When the external magnetic field was applied along the axis of the ring, under the effect of the magnetic induction, the current to flow in each half of the ring, this current lags with respect to external magnetic field thereby giving a strong magnetic response. Besides, field patterns were

exhibited in Fig. 3(a-c). Therefore, it can be stated that the square split resonator mainly causes electric and magnetic polarities. The surface current distribution on the metamaterial structure was shown in Fig. 3(d), where it is easy to find that the direction of the currents on the inner and outer resonator. The directions of the currents were opposite on the inner and outer resonators at the resonance frequencies. This means the presented anti-phase feeding structure used to feeding the array was very effective. The colour indicates the intensity of the currents. On the other hand, the arrows show the directions of the current.

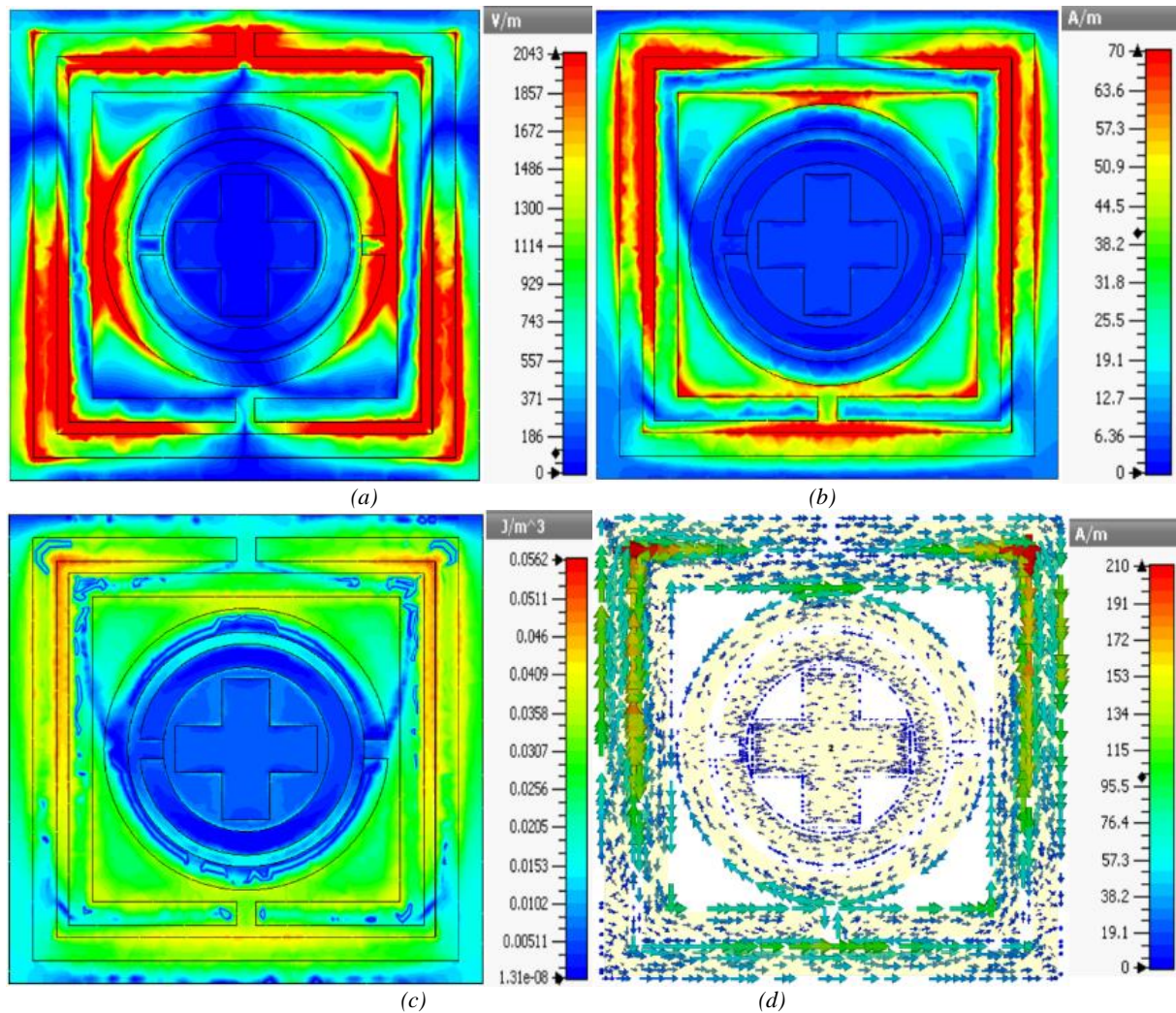


Fig. 3. (a) Electric field pattern, (b) Magnetic field pattern, (c) Electric energy density and (d) Surface current distribution of the designed metamaterial absorber at 4.12 GHz (color online)

The EM-characteristics of the metamaterial absorber can be described by the reflection (S_{11}) and transmission (S_{21}) coefficient, which can be represented in many forms like, Scattering parameters, impedance, etc. From figure 4(a) there are four passing windows displayed, and the passing windows were respectively at C-, X- and Ku-bands. Moreover, the measurement was done for the experimental validation, and the measured and simulated results were well suited together. The simulated result shows transmittance (S_{21}) resonance at 4.13 GHz (C-band), 8.19 GHz (X-band), 12.01 GHz (Ku-band) and 16.63 GHz (Ku-band). In addition, the measured results were 4.16 GHz (C-band), 8.18 GHz (X-band), 12.03 GHz (Ku-band), and 16.61 GHz (Ku-band) in Fig. 4(a). In addition, from figure 4(b), the reactance impedance was $-69.14-27.27i$ at 9.39 GHz. In Fig. 4(c), negative permittivity was achieved at four frequency ranges. The first one was approximately from 3.29 to 4.64 GHz, while the second, third, and the last one was from 5.64 to 8.50 GHz, 9.16 to 11.55 GHz, 12.83 to 13.94 GHz, respectively. Further, the negative permeability was

achieved from 9.20 to 18.0 GHz. Moreover, the negative refractive index also achieved at three frequency ranges. The first one was around 5.80 to 7.94 GHz which covers 2.14 GHz frequency bandwidth, whereas the second and the third one was from 9.42 to 14.08 GHz, and 16.48 to 18.0 GHz, respectively where they cover 4.66 and 1.52 GHz frequency bandwidth, respectively. Therefore, the designed structure can be called as a left-handed metamaterial absorber for any frequency peaks between 9.42 to 11.55 GHz. The absorption of the designed absorber was evaluated from equation 8. The absorption of the proposed absorber at reflection (S_{11}) resonance point was shown in Fig. 4(d) and Table 1. So, the absorption rate at 2.06, 5.05, 9.26, and 13.23 GHz were 60%, 95%, 78%, and 93%, respectively

Table 1. Absorption peaks of the designed absorber

Resonance of S_{11} (GHz)	2.06	5.05	9.26	13.23
Absorption	60%	95%	78%	93%

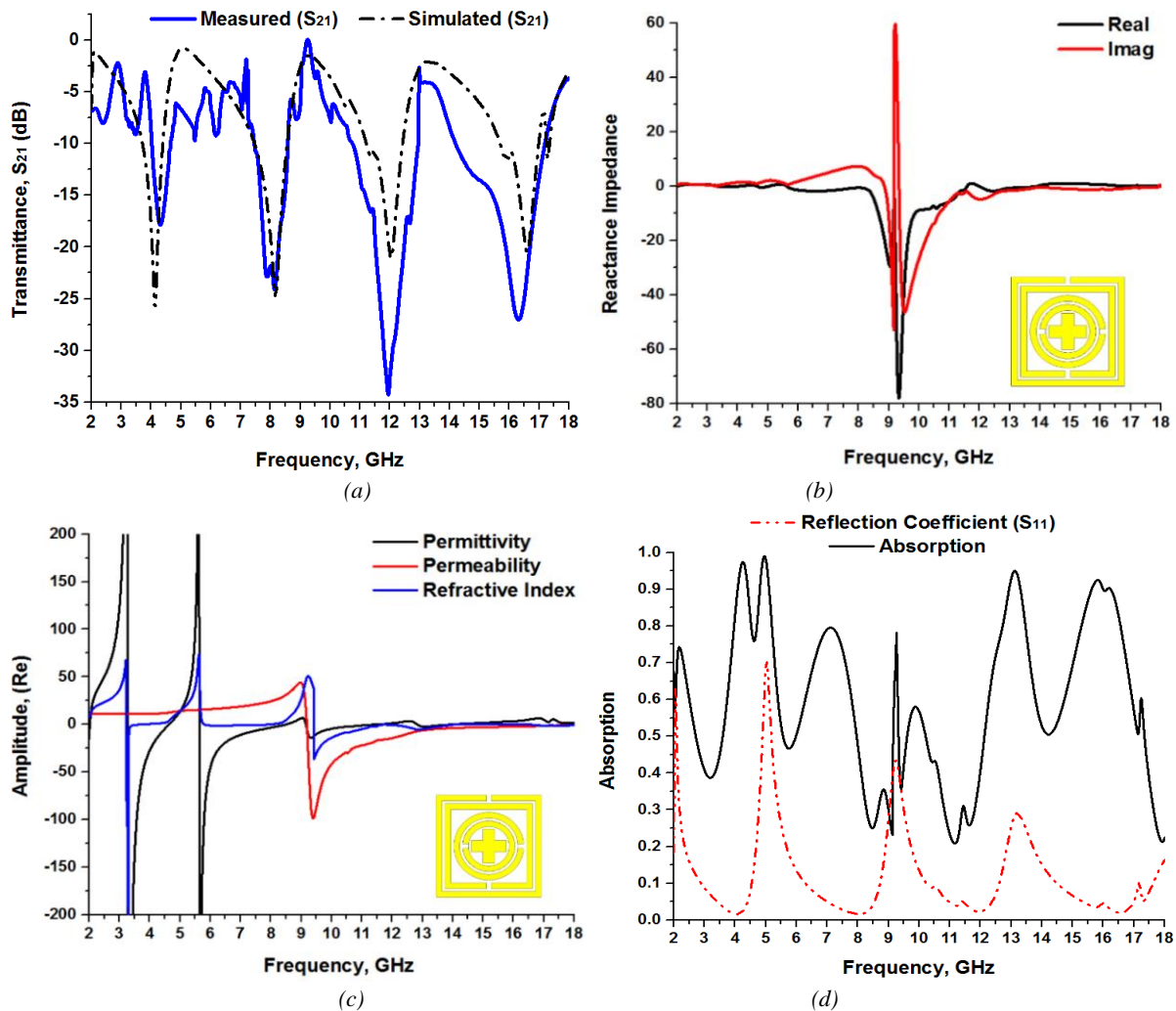


Fig. 4. (a) Measured and simulated transmittance, (b) Reactance impedance, (c) Effective medium parameters, and (d) Absorption peaks (color online)

Table 2 depicts a comparison between the designed energy harvester and the reported researches in the introduction section. From the table, the proposed structure is compact and flexible than the reported other studies. The proposed structure is only $10 \times 10 \text{ mm}^2$, whereas in ref. [2, 7, 11 and 14] are respectively $15 \times 15 \text{ cm}^2$, $15 \times 15 \text{ mm}^2$, $85 \times 85 \text{ mm}^2$ and $13 \times 13 \text{ mm}^2$ - moreover, ref. [5] is more miniature than the proposed absorber, but it is not applicable for GHz frequency range only for the THz frequency range. In addition, the harvested energy from the ref. [3, 6, 7, 11 and 14] are respectively 88%, 96%, 55%, 78%, and 93%. Here ref. [6] is only for terahertz frequency range and rest all of the references are for the gigahertz frequency range - absorption of ref. [14] is similar to the designed absorber, but the harvester size is bigger than the proposed one.

Table 2. Performance comparison of the proposed harvester with the reported researches

Ref. No.	Structure Size	Absorption
Landy et al. [3]	$15 \times 15 \text{ cm}^2$	88%
Wang et al. [6]	$210 \times 210 \mu\text{m}^2$	96%
Islam et al. [7]	$15 \times 15 \text{ mm}^2$	55%
Ramahi et al. [11]	$85 \times 85 \text{ mm}^2$	78%
Almoneefa et al. [14]	$13 \times 13 \text{ mm}^2$	93%
Proposed Absorber	$10 \times 10 \text{ mm}^2$	93%

5. Conclusion

A metamaterial absorber was formed by the combination of an electrical resonator, and a circular ring was introduced in this paper. For the experimental validation, the measurement was done. The absorber structure showed a wide bandwidth of 4.66 GHz and resonance frequency peaks in C-, X- and Ku-band. The effective medium ratio is 7.21, and the absorption capacity of the proposed absorber was 95%. Due to the high absorption capacity, the proposed absorber can save

human life from the unwanted electromagnetic radiation in space/environment as well as can convert absorbed undesirable radiation to power for energy harvesting applications.

Acknowledgements

The Research Universiti Grant Geran Universiti Penyelidikan (GUP), code: 2018-134 supported this work.

References

- [1] J. W. Norbury, K. M. Maung, *Acta Astronautica* **60**, 770 (2007).
- [2] H. C. Van De Hulst, *Electromagnetic Radiation in Space*, Springer, Verlag, p. 1, 1967
- [3] N. I. Landy, S. Sajuyigbe, J. J. Mock, D. R. Smith, W. J. Padilla, *Physical Review Letters* **100**, 1 (2008).
- [4] M. R. I. Faruque, M. T. Islam, *Progress in Electromagnetics Research* **141**, 463 (2013).
- [5] M. R. I. Faruque, M. M. Hasan, M. T. Islam, *Appl. Phys. A* **124**, 127 (2018).
- [6] B.-X. Wang, *IEEE Journal of Quantum Electronics* **23**(4), (2017).
- [7] S. S. Islam, M. R. I. Faruque, M. T. Islam, *Science Engineering Composite Mater* **10**(24), 139 (2017).
- [8] N. Wang, J. Tong, W. Zhou, W. Jiang, J. Li, X. Dong, S. Hu, *IEEE Photonics Journal* **7**(1), 5500506 (2015).
- [9] M. M. Hasan, M. R. I. Faruque, M. T. Islam, *Microwave and Optical Technology Letters* **59**, 1772 (2016).
- [10] L. M. Swallow, J. K. Luo, E. Siores, I. Patel, D. Dodds, *Smart Materials and Structures* **17**, 025017 (2008).
- [11] O. M. Ramahi, T. S. Almoneef, M. Alshareef, M. S. Boybay, *Applied Physics Letters* **101**, 173903 (2012).
- [12] H. Wang, V. P. Sivan, A. Mitchell, G. Rosengarten, P. Phelan, L. Wang, *Solar Energy Materials & Solar Cells* **137**, 235 (2015).
- [13] M. M. Hasan, M. R. I. Faruque, M. T. Islam, *Microwave and Optical Technology Letters* **59**(9), 2302 (2017).
- [14] T. S. Almoneefa, O. M. Ramahib, *Applied Physics Letters* **106**, 153902 (2015).
- [15] Y. Cheng, Y. Zou, H. Luo, F. Chen, X. Mao, *Journal of Electronic Materials* **48**(6), 3939 (2019).
- [16] Q. Wang, Y. Cheng, *AEU-International Journal of Electronics and Communications* **120**, 153198 (2020).
- [17] H. Zou, Y. Cheng, *Optical Materials* **88**, 674 (2019).
- [18] F. Chen, Y. Cheng, H. Luo, *Materials* **13**(4), 860 (2020).
- [19] F. Chen, Y. Cheng, H. Luo, *IEEE Access* **8**, 82981 (2020).
- [20] W. Li, Y. Cheng, *Optics Communications* **462**, 125265 (2020).
- [21] M. M. Hasan, M. R. I. Faruque, M. T. Islam, *Materials Research Express* **4**, 035015 (2017).

* Corresponding author: rashed@ukm.edu.my